

# Time-dependent modelling of ELMing H-mode at TCV with SOLPS5

B. Gulejová, R.A. Pitts, X. Bonnin<sup>1</sup>, D. Coster<sup>2</sup>, R. Behn, J. Horáček<sup>3</sup>, J. Marki

and the TCV Team

*École Polytechnique Fédérale de Lausanne (EPFL), Centre de Recherches en Physique des Plasmas,  
Association Euratom – Confédération Suisse, 1015 Lausanne, Switzerland*

<sup>1</sup>*LIMHP, CNRS-UPR, Université Paris 13, 99 av JB Clement, 93430 Villetaneuse, France*

<sup>2</sup>*Max-Planck Institut für Plasmaphysik, EURATOM-Association, Garching, Germany*

<sup>3</sup>*Institute of Plasma Physics, v.v.i., Association EURATOM-IPP.CR, Prague, Czech Republic*

## Introduction

The threat of intolerable divertor damage in ITER and future tokamak reactors caused by edge localized modes (ELMs) has lately made their transport in the scrape-off layer (SOL) the subject of considerable research activity [1]. This contribution describes work which builds on the recent first successful attempts at modelling the inter-ELM phase of TCV Type III ELMing ohmic H-modes using the coupled fluid-Monte Carlo SOLPS5 code [2]. These simulations have now been extended to include a time dependent model, allowing ELMs to be described. Compared with the larger Type I ELMs commonly studied elsewhere, the Type III ELM that will be discussed here is a small event in terms of stored energy loss ( $\Delta W_{\text{ELM}}/W \sim 2\%$ ) and absolute energy ( $\Delta W_{\text{ELM}} \sim \text{few } 100 \text{ J}$ ). It is therefore perhaps more appropriate to the necessarily fluid approximation required for a description with SOLPS5 code. Here the emphasis will be on matching upstream Thomson Scattering (TS) measurements of the  $T_e$  and  $n_e$  profile evolution during the ELM cycle and comparing with particle fluxes at the outer divertor target from Langmuir probe (LP) measurements on the ELM timescale.

## Experiment

Typical single null lower (SNL) ohmic Type III ELMing H-mode discharges at TCV have plasma current in the range  $I_p = 350 - 430 \text{ kA}$ ,  $\bar{n}_e \sim 5 \times 10^{19} \text{ m}^{-3}$  ( $n/n_{\text{GW}} \sim 0.3$ ) and  $\sim 1 \text{ s}$  steady-state ELMing phases with  $f_{\text{ELM}}$  which can vary from 100-200 Hz, and where each ELM exhausts typically  $\sim 0.5 \text{ kJ}$  of plasma stored energy ( $W_{\text{dia}} \sim 20 \text{ kJ}$  for these plasmas). More details can be found in [2]. Unfortunately since not all required diagnostics are available at the required time resolution in any given shot, signals from discharges have been combined for comparisons with the simulations. The target discharge #26730 has been used to simulate the inter-ELM pedestal and SOL plasma (see [2]) using coherently averaged upstream core and edge Thomson Scattering (TS) data. In this paper, TS data from the very similar discharge #26393 is used to benefit from the fast consecutive pulsing of the TS lasers which allows two pedestal profiles to be measured in quick succession ( $\sim 1 \text{ ms}$ ) during the same ELM (see [3] and Fig. 1 a) below).

## Time-dependent simulation of the ELM

There is currently no convincing ELM model describing how energy released from the edge pedestal is transferred to the divertor targets. It is likely, though not yet proven, that the mechanism involves a magnetic reconnection process by which hot pedestal plasma on closed field lines can reach the targets via parallel transport. In SOLPS5, the only method currently available to simulate this process is to increase the diffusive heat and particle transport

coefficients used to simulate the pre-ELM state for the ELM duration,  $t_{ELM}$ , such that the total energy expelled during this time is compatible with that measured experimentally. Assuming no velocity pinch term, this may be expressed approximately as

$$\frac{E_{ELM}}{2.t_{ELM}.A_{ELM}} = -n.\frac{dT}{dr}.\chi_{\perp} - \frac{5}{2}.T.\frac{dn}{dr}.D_{\perp}$$

with  $A_{ELM}$  the separatrix area over which the ELM is released. Here a Gaussian poloidal distribution centred on the outside midplane has been applied and different multiplying factors of the pre-ELM transport coefficients  $D_{\perp}$ ,  $\chi_{\perp}$  chosen such that  $E_{ELM}$  approximately matches the measured  $\Delta W_{ELM}$  for a typical ELM in the discharge. In addition to the magnitude increase, the shape of the  $D_{\perp}$  and  $\chi_{e,i}$  profiles must also be modified compared with the pre-ELM values to account for the collapse of the edge transport barrier (ETB) and provide the best match to TS and target LP data. Time-dependent ELM simulations require the Monte-Carlo neutral code (EIRENE) to be run with time steps,  $dt$  equivalent to those of the fluid code (B2.5) to avoid artificial compression of the neutral timescale [4]. Here,  $dt = 10^{-6}$  s has been chosen, providing 100 points during the ELM. Thus far only a single ELM cycle has been simulated, covering a total time of 400  $\mu$ s, with 100  $\mu$ s before and 200  $\mu$ s after. All charge states of carbon are included in these simulations and no drift terms are activated. Heat flux limiters are set at 10 for ions and 0.3 for electrons, unchanged through the ELM cycle.

## Results and comparison with experiment

Fig. 1 a) compares pedestal and target profiles from experiment and simulation in the pre-ELM phase and after the ELM crash when the pedestal has relaxed. From experiment, a coherent average of the stored energy derived from a diamagnetic loop over 40 ELMs during the stationary phase of the discharge yields  $\Delta W_{ELM} \sim 600$  J (2.5% of total plasma stored energy). For the ELM duration, a value of  $t_{ELM} \sim 100$   $\mu$ s is estimated from the phase of turbulent activity on Mirnov coils located on the outboard midplane wall. Assuming  $A_{ELM} \sim 1.5$  m<sup>2</sup>,  $D_{\perp}$  and  $\chi_{e,i}$  are increased across the whole radial profile from pedestal top to edge of the simulation grid in the SOL such that the expelled energy in the simulation is 620 J, close to the experimental value. Of this 620 J SOLPS5 finds 55% of it at the divertor targets. Upstream, the experimental profiles show a larger drop in  $n_e$  than  $T_e$  at the pedestal top (a feature which is even more pronounced in the coherently averaged TS profiles shown in [3]), indicating that this ELM is more convective than conductive (i.e. that  $\langle T_{e,ped} \rangle \Delta n_{e,ped}$  exceeds  $\langle n_{e,ped} \rangle \Delta T_{e,ped}$  in the contribution to  $\Delta W_{ELM}$ ). For this reason  $D_{\perp}$  has been increased more during the ELM than  $\chi_{e,i}$  in the simulation. In fact,  $D_{\perp}$  is increased everywhere by 100 times, with  $\chi_{e,i}$  being increased mostly in the pedestal region (by a factor 10) and only by  $\sim$ factor 2 in the SOL.

At the outer target SOLPS5 ELM and pre-ELM profiles are compared in Fig. 1 b) with coherently averaged data (40 ELMs between  $t = 0.6$  and  $0.8$  s) for the ion particle fluxes (the ion saturation fluxes to tile embedded LPs). Measurements of  $T_e$  at the target are not possible on the ELM timescale and so only SOLPS5 results are shown in this case. Similarly, although fast surface power fluxes are now becoming available on TCV [5], there are no measurements for the particular discharge type described here. The SOLPS5 power flux profile in Fig. 1 b)

has been computed assuming a sheath heat transmission factor of  $\gamma = 7.5$ . Agreement with experimental particle fluxes is fair in magnitude ( $\sim$  factor 2) and good in profile shape. The peak target electron temperatures in Fig. 1b are high, similar to the pedestal values and considerably higher ( $\sim$  factor 3) than the very approximate estimates made in [6] on the basis of coherent averaging and combination of LP signals. Only when IR data become available will it be possible to further benchmark these SOLPS5 results involving particle energy and not simply flux.

Fig.2 describes the simulated time dependence of the upstream and downstream separatrix  $T_i$ ,  $T_e$  and the strike point perpendicular power flux density. As mentioned above, there is very little drop in  $T_e$  along the  $\sim 18$  m of parallel connection length from upstream to target. However,  $T_i$  decreases about 4.5 times from midplane to the target, indicating strong ion cooling. The time evolution of  $T_e$ ,  $T_i$  and power flux at the target is quite similar to that reported from 1D kinetic particle-in-cell (PIC) simulations of ELM parallel heat propagation [7,8]. In common with the PIC simulations, the target power flux rises on the ion and not the electron timescale. Beyond  $t_{ELM}$ , there is an abrupt decrease in  $T_e$  on the  $1 \mu s$  timescale (the approximate electron thermal transit time from upstream to pedestal). Some  $10 \mu s$  later,  $T_i$  begins to fall. This is significantly faster than expected on the basis of ion sonic transit time ( $\sim L_{\parallel}/c_s \sim 150 \mu s$ ). Strong e-i collisional coupling and the possibility of Monte-Carlo noise in the neutral simulations maybe responsible for some of this discrepancy. Studies are underway to investigate this. It is notable however that  $T_i$  at the target rises on a much slower timescale than its increase at the ELM onset.

## Conclusion

Time dependent simulations of TCV ELMs have begun with SOLPS5. Preliminary results are encouraging in terms of absolute agreement with experimental upstream and target measurements, but more work is required to understand discrepancies in the time evolution of target electron and ion temperatures. The ELM is inherently a kinetic event and simulations with the BIT1 code [7] are planned for these TCV ELMs in order to provide comparison with the fluid simulations.

## Acknowledgement

This work was funded in part by the Swiss National Science Foundation. JH acknowledges support from the European Atomic Energy Community under an intra-European fellowship.

## References

- [1] A. Loarte et al., Physica Scripta **T128** (2007) 222
- [2] B. Gulejova et al., J. Nucl. Mater. **363-365** (2007) 1037
- [3] R. Behn et al., accepted for publication in Plasma Phys. Control. Fusion (2007)
- [4] D. P. Coster, in : Proc. of 30<sup>th</sup> EPS, St. Petersburg, ECA **27A**, P-1.169 (2003)
- [5] J. Marki et al., 34<sup>th</sup> EPS, Warsaw (2007)
- [6] R. A. Pitts et al., Nucl. Fusion **43** (2003) 1145
- [7] D. Tskhakaya et al, 34<sup>th</sup> EPS, Warsaw (2007)
- [8] R. A. Pitts et al., IAEA 2006, Paper EX/3-1, submitted to Nucl. Fusion (2007)

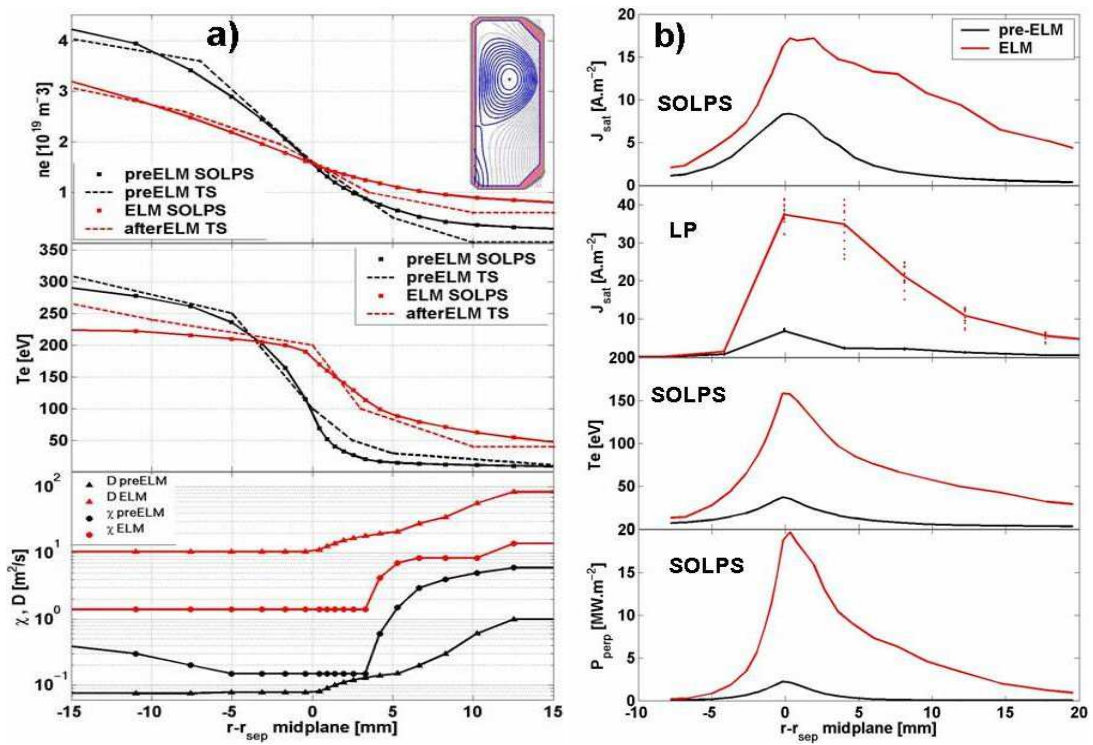


**Fig.1:** a) Upstream  $n_e$ ,  $T_e$  profiles from SOLPS and TS (#26393) measured before and after ELM (TS data extracted from [4]) and transport coefficients  $D$ ,  $\chi_{e,i}$  used in SOLPS for pre-ELM and ELM. The inset shows the TCV equilibrium reconstruction appropriate to the shot described here. b) Pre-ELM and ELM outer target profiles of  $j_{\text{sat}}$  from SOLPS compared with  $j_{\text{sat}}$  from LPs (#26730) and  $T_e$  and  $\Gamma_{\text{perp}}$  from SOLPS

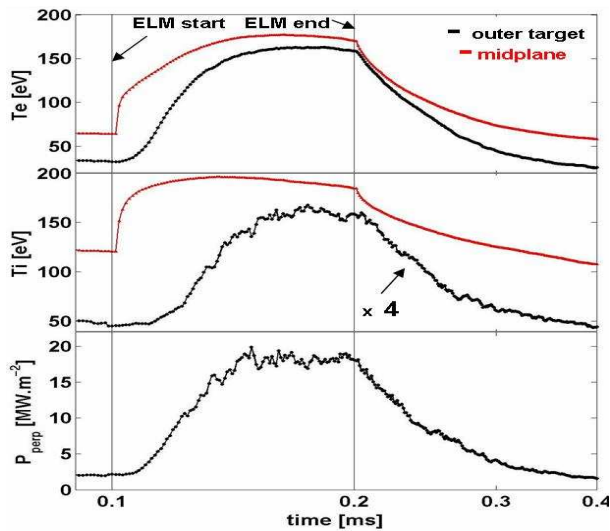


**Fig.2:** Time evolution of the upstream and outer target separatrix SOLPS  $T_e$ ,  $T_i$  and outer strike point perpendicular power flux density through the simulated ELM cycle.